Tunable thermal wave nonreciprocity by spatiotemporal modulation

Liujun Xu,[1,*] Jiping Huang,[1,†] and Xiaoping Ouyang[2,‡]
[1]Department of Physics, State Key Laboratory of Surface Physics, and Key Laboratory of Micro and Nano Photonic Structures (MOE), Fudan University, Shanghai 200438, China
[2]School of Materials Science and Engineering, Xiangtan University, Xiangtan 411105, China

(Received 10 December 2020; revised 22 January 2021; accepted 24 February 2021; published 18 March 2021)

Nonreciprocity is of particular importance to realize one-way propagation, thus attracting intensive research interest in various fields. Thermal waves, essentially originating from periodic temperature fluctuations, are also expected to achieve one-way propagation, but the related mechanism is still lacking. To solve the problem, we introduce spatiotemporal modulation to realize thermal wave nonreciprocity. Since thermal waves are completely transient, both the convective term and the Willis term induced by spatiotemporal modulation should be considered. We also analytically study the phase difference between two spatiotemporally modulated parameters, which offers a tunable parameter to control nonreciprocity. We further define a rectification ratio based on the reciprocal of spatial decay rate and discuss nonreciprocity conditions accordingly. Finite-element simulations are performed to confirm theoretical predictions, and experimental suggestions are provided to ensure the feasibility of spatiotemporal modulation. These results have potential applications in realizing thermal detection and thermal stabilization simultaneously.

DOI: 10.1103/PhysRevE.103.032128

I. INTRODUCTION

Ever since the concept of spatiotemporal modulation was proposed [1], intensive studies have been conducted not only in wave systems [2–16] including photonics [2–5], acoustics [6–9], and metasurfaces [10–12] but also in diffusion systems [17–19]. A direct application of spatiotemporal modulation is to realize nonreciprocity which refers to asymmetric propagation along opposite directions. Although many different kinds of waves have been studied to achieve nonreciprocity based on spatiotemporal modulation, thermal waves have received little attention despite an important phenomenon. In terms of mechanism, thermal waves are a special kind of waves, which are dominated by a diffusion equation (i.e., the Fourier equation), thus also called diffusion waves [20]. In terms of application, thermal waves can realize nondestructive detection (i.e., thermal wave imaging) which is widely applied in aerospace, machinery, and electricity [21–23]. Some recent studies also focused on diffusion waves to realize anti-parity-time symmetry [24–27], negative thermal transport [28], cloaks [20,29–31], and crystals [32–34].

However, a mechanism to achieve thermal wave nonreciprocity is still lacking. Essentially, thermal waves can be treated as periodic temperature fluctuations which are usually a double-edged sword. On the one hand, they are desirable for thermal detection. On the other hand, they are unwanted for thermal stabilization. Therefore, it is crucially important to realize thermal wave nonreciprocity. For this purpose, we explore spatiotemporal modulation to achieve thermal wave nonreciprocity, inspired by pioneering studies on nonreciprocal thermal materials [18]. It has been revealed that a convective term appears in the conduction equation at quasisteady states if thermal conductivity and mass density are spatiotemporally modulated, thus achieving nonreciprocity. However, the applicability for thermal waves was not discussed. On the one hand, thermal waves feature completely transient states where the Willis term should be considered. On the other hand, the phase difference between two spatiotemporally modulated parameters remains to be explored.

In this work, we fully discuss thermal wave nonreciprocity based on spatiotemporal modulation. Since there is a phase difference between two spatiotemporally modulated parameters, we construct two different backward cases (see Fig. 1) which have different nonreciprocity conditions. The results demonstrate that the phase difference offers a flexible and tunable parameter to control nonreciprocity. We also discuss the heat flux to reveal the feature of spatiotemporal modulation.

II. THEORY

We consider a passive thermal conduction process in one dimension, dominated by

$$\rho(x-ut)\frac{\partial T}{\partial t}+\frac{\partial}{\partial x}\left[-\sigma(x-ut)\frac{\partial T}{\partial x}\right]=0, \tag{1}$$

where $\sigma(x-ut)$ is thermal conductivity and $\rho(x-ut)$ is the product of mass density and heat capacity. The spatiotemporally modulated parameters in Fig. 1(a) take the form of

$$\sigma(x-ut)=\sigma_A+\sigma_B\cos[K(x-ut)], \tag{2a}$$

$$\rho(x-ut)=\rho_A+\rho_B\cos[K(x-ut)+\alpha], \tag{2b}$$

[*]13307110076@fudan.edu.cn
[†]jphuang@fudan.edu.cn
[‡]oyxp2003@aliyun.com

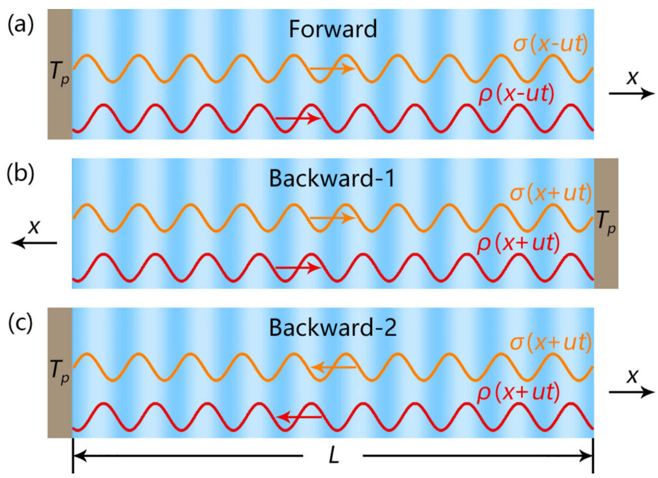

FIG. 1. Thermal wave nonreciprocity. (a) Forward case. (b) Backward-1 case by changing the source position. (c) Backward-2 case by changing the modulation direction.

where σ_A, σ_B, ρ_A, and ρ_B are four constants. $K = 2\pi/\gamma$ is wave number, γ is wavelength, u is modulation speed, and α is phase difference. Since $\sigma(x-ut)$ and $\rho(x-ut)$ are periodic functions, the Bloch theorem is applicable and the temperature solution can be expressed as

$$T = \phi(x-ut)e^{i(kx-\omega t)}, \tag{3}$$

where k and ω are, respectively, the wave number and circular frequency of a thermal wave. $\phi(x-ut)$ is an amplitude modulation function that has the same periodicity as $\sigma(x-ut)$ and $\rho(x-ut)$. Equation (1) can then be homogenized with the approximations of $k \ll K$ and $\omega \ll uK$ [18],

$$\tilde{\rho}\frac{\partial \tilde{T}}{\partial t} + C\frac{\partial \tilde{T}}{\partial x} - \tilde{\sigma}\frac{\partial^2 \tilde{T}}{\partial x^2} - S\frac{\partial^2 \tilde{T}}{\partial x \partial t} = 0, \tag{4}$$

where the homogenized parameters can be expressed as

$$\tilde{\sigma} \approx \sigma_A\left(1 - \frac{\sigma_B^2}{2\sigma_A^2}\frac{1}{1+\Gamma^2}\right), \tag{5a}$$

$$\tilde{\rho} \approx \rho_A\left(1 - \frac{\rho_B^2}{2\rho_A^2}\frac{\Gamma^2}{1+\Gamma^2}\right), \tag{5b}$$

$$C \approx u\frac{\sigma_B\rho_B}{2\sigma_A}\frac{1}{1+\Gamma^2}P(\alpha), \tag{5c}$$

$$S \approx \frac{1}{u}\frac{\sigma_B\rho_B}{2\rho_A}\frac{\Gamma^2}{1+\Gamma^2}Q(\alpha), \tag{5d}$$

with $\Gamma = \rho_A u\gamma/(2\pi\sigma_A)$, $P(\alpha) = \cos\alpha + \Gamma\sin\alpha$, and $Q(\alpha) = \cos\alpha + \Gamma^{-1}\sin\alpha$. $\tilde{T}$ can be treated as the envelope line of the actual temperature T. Here, we extend the results reported in Ref. [18] by additionally considering a phase difference of α, and the detailed derivations can be found in the Appendix. $\tilde{\sigma}$ and $\tilde{\rho}$ are irrelevant to α, but C and S are dependent on α, offering a tunable parameter.

We then qualitatively discuss the nonreciprocity induced by spatiotemporal modulation. In what follows, the subscripts of f, $b1$, and $b2$ denote the parameters related to the forward case in Fig. 1(a), the backward-1 case in Fig. 1(b), and the backward-2 case in Fig. 1(c), respectively. The two backward cases are equivalent only when $\alpha = 0$. Since $\tilde{\sigma}$ and $\tilde{\rho}$ do not contribute to nonreciprocity, we mainly discuss C and S in detail.

For the forward case, we know $C_f = C$ and $S_f = S$. For the backward-1 case, we can derive $C_{b1} = -C$ and $S_{b1} = -S$. Nonreciprocity requires $C_f \neq C_{b1}$ (or $S_f \neq S_{b1}$). Therefore, as long as $C \neq 0$ (or $S \neq 0$), nonreciprocity will occur and a larger C (or S) yields larger nonreciprocity. For clarity, we plot the functions of $C(\alpha)$ and $S(\alpha)$ in Fig. 2 with $\Gamma = 0.5,\ 1,\ 2$. The maximum and minimum values of C appear at $\alpha = -\mathrm{arccot}\Gamma + \pi/2$ and $\alpha = -\mathrm{arccot}\Gamma - \pi/2$, respectively; and the zero value occurs at $\alpha = \arctan\Gamma \pm \pi/2$. The maximum and minimum values of S appear at $\alpha = -\arctan\Gamma + \pi/2$ and $\alpha = -\arctan\Gamma - \pi/2$, respectively; and the zero value occurs at $\alpha = \mathrm{arccot}\Gamma \pm \pi/2$. For the backward-2 case, we can obtain $C_{b2} = C(-u)$ and $S_{b2} = S(-u)$. Nonreciprocity requires $C_f \neq C_{b2}$ (or $S_f \neq S_{b2}$). Therefore, as long as $C(u) \neq C(-u)$ [or $S(u) \neq S(-u)$], nonreciprocity will occur. We can also observe that $\alpha = \pm\pi/2$ makes $P(\alpha)$ and $Q(\alpha)$ two odd functions of u. C and S then become two even functions of u, so nonreciprocity disappears. In one word, the nonreciprocity condition for the backward-1 case is $C \neq 0$ (or $S \neq 0$), and that for the backward-2 case is $C(u) \neq C(-u)$ [or $S(u) \neq S(-u)$]. Especially when $\alpha = 0$, $C(-u) = -C(u)$ [or $S(-u) = -S(u)$], the nonreciprocity condition for the backward-2 case can then be reduced to $C \neq 0$ (or $S \neq 0$), which is the same as that for the backward-1 case.

We then consider a transient case which can support the propagation of thermal waves. Since both C and S can contribute to nonreciprocity, a qualitative analysis is not enough. Therefore, we quantitatively discuss a rectification ratio. For this purpose, we apply a periodic temperature at the left side of the structure in Fig. 1(a) to generate a forward thermal wave described by Eq. (3). The periodic temperature has a form of $T_p = \phi_0 e^{-i\omega t} + T_0$ where ϕ_0 denote the temperature amplitude. We set the reference temperature $T_0 = 0$ K in theoretical discussions for brevity. The envelope line of the actual temperature T can then be expressed as

$$\tilde{T} = \phi_0 e^{i(kx-\omega t)}. \tag{6}$$

The real part of Eq. (6) makes sense, which has been experimentally realized by periodically heating a material [24,25]. The substitution of Eq. (6) into Eq. (4) yields

$$-i\omega\tilde{\rho} + ikC + k^2\tilde{\sigma} - \omega k S = 0. \tag{7}$$

Since thermal conduction features dissipation, the wave number k should be complex, i.e., $k = \mu + i\xi$ with μ and ξ being two real numbers. Equation (6) can then be rewritten as $\tilde{T} = \phi_0 e^{-\xi x}e^{i(\mu x - \omega t)}$. Therefore, the physical meaning of μ is the wave number and that of ξ is the spatial decay rate. With the complex k, Eq. (7) can be further reduced to

$$-i\omega\tilde{\rho} + i(\mu+i\xi)C + (\mu+i\xi)^2\tilde{\sigma} - \omega(\mu+i\xi)S = 0. \tag{8}$$

By independently considering the real and imaginary parts of Eq. (8), we can derive two equations,

$$-\xi C + (\mu^2 - \xi^2)\tilde{\sigma} - \omega\mu S = 0, \tag{9a}$$

$$\omega\tilde{\rho} - \mu C - 2\mu\xi\tilde{\sigma} + \omega\xi S = 0. \tag{9b}$$

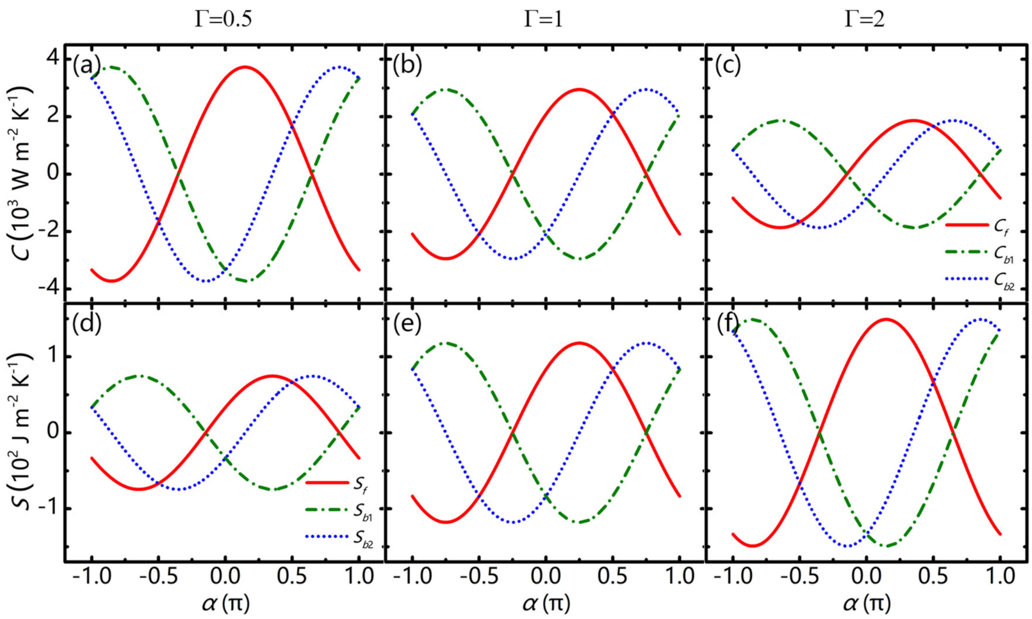

FIG. 2. C and S as functions of α. Parameters: $\sigma_A = 300$ W m^{-1} K^{-1}, $\sigma_B = 100$ W m^{-1} K^{-1}, $\rho_A = 3 \times 10^6$ J m^{-3} K^{-1}, $\rho_B = 5 \times 10^5$ J m^{-3} K^{-1}, and $u = 0.05$ m/s.

The solution to Eq. (9) is

$$\mu = \frac{2S\omega + \sqrt{2}\varepsilon}{4\tilde{\sigma}}, \tag{10a}$$

$$\xi = \frac{-4C\omega(2\tilde{\sigma}\tilde{\rho} - CS) + 2\sqrt{2}(C^2 - S^2\omega^2)\varepsilon + \sqrt{2}\varepsilon^3}{8\tilde{\sigma}(2\tilde{\sigma}\tilde{\rho} - CS)\omega}, \tag{10b}$$

with $\varepsilon = \sqrt{-C^2 + S^2\omega^2 + \sqrt{(C^2 + S^2\omega^2)^2 + 16\omega^2\tilde{\sigma}\tilde{\rho}(\tilde{\sigma}\tilde{\rho} - CS)}}$. Although Eq. (10) is complicated, we can discuss some special conditions to have a rough idea. For the forward case, we can know $\mu_f = \mu$ and $\xi_f = \xi$. For the backward-1 case, we can derive $\mu_{b1} = \mu(-C, -S)$ and $\xi_{b1} = \xi(-C, -S)$. Due to $\varepsilon(C, S) = \varepsilon(-C, -S)$, it does contribute to nonreciprocity, so the nonreciprocity origins of μ and ξ lie in S and C, respectively [see Eq. (10)]. We can then conclude that nonreciprocal μ requires $S \neq 0$ (i.e., $\alpha \neq \text{arccot}\Gamma \pm \pi/2$) and nonreciprocal ξ requires $C \neq 0$ (i.e., $\alpha \neq \arctan\Gamma \pm \pi/2$). For the backward-2 case, we can derive $\mu_{b2} = \mu[C(-u), S(-u)]$ and $\xi_{b2} = \xi[C(-u), S(-u)]$. When $\alpha = \pm\pi/2$, C, S, and ε are all even functions of u, so nonreciprocity will disappear. Therefore, nonreciprocal μ (or ξ) requires $\alpha \neq \pm\pi/2$.

In general, it makes little sense to define a rectification ratio based on wave numbers. However, it is meaningful to define a rectification ratio (R_T) based on the temperature amplitude ($\phi_0 e^{-\xi x}$) or the reciprocal of spatial decay rate ($1/\xi$),

$$R_{T1} = \frac{1/\xi_f - 1/\xi_{b1}}{1/\xi_f + 1/\xi_{b1}} = \frac{\xi_{b1} - \xi_f}{\xi_{b1} + \xi_f}, \tag{11a}$$

$$R_{T2} = \frac{1/\xi_f - 1/\xi_{b2}}{1/\xi_f + 1/\xi_{b2}} = \frac{\xi_{b2} - \xi_f}{\xi_{b2} + \xi_f}, \tag{11b}$$

where R_{T1} and R_{T2} are defined for the backward-1 and backward-2 cases, respectively. We plot R_{T1} and R_{T2} as functions of α in Fig. 3. The results demonstrate that a smaller Γ or a smaller ω yields larger nonreciprocity. Therefore, both R_{T1} and R_{T2} can theoretically reach 1, and we can obtain a perfect thermal wave diode. Especially when $\alpha = 0$, Eq. (11) can be reduced to

$$R_{T1} = R_{T2} = \frac{2\sqrt{2}C\omega(2\tilde{\sigma}\tilde{\rho} - CS)}{2(C^2 - S^2\omega^2)\varepsilon + \varepsilon^3}, \tag{12}$$

indicating that the two backward cases are equivalent when $\alpha = 0$.

Another possibility to define a rectification ratio (R_J) lies in nonreciprocal heat fluxes J. For this purpose, we define the dynamic heat flux J according to Eq. (1),

$$\begin{aligned} J &= -\sigma(x - ut)\frac{\partial T}{\partial x} \\ &= -\sigma(x - ut)\frac{\partial}{\partial x}[\phi(x - ut)e^{-\xi x}e^{i(\mu x - \omega t)}] \\ &= -\sigma(x - ut)[\phi'(x - ut) \\ &\quad + (-\xi + i\mu)\phi(x - ut)]e^{-\xi x}e^{i(\mu x - \omega t)}, \end{aligned} \tag{13}$$

where $\phi'(x - ut) = \partial\phi(x - ut)/\partial x$. Since $\sigma(x - ut)$, $\phi(x - ut)$, and $\phi'(x - ut)$ are all periodic functions, the dynamic heat flux described by Eq. (13) varies with temporal periodicity, but the heat flux amplitude decays along the x axis due to the term of $e^{-\xi x}$. Therefore, we can also define R_J based on the reciprocal of spatial decay rate ($1/\xi$) which should have the same form as Eq. (11), indicating that the whole theoretical framework is self-consistent.

We can then draw a brief conclusion. Spatiotemporal modulation can generate two additional terms including the convective term associated with C and the Willis term related to S. Both C and S can be flexibly tuned by α. We also discuss two backward cases: (i) changing the source position and (ii) changing the modulation direction, which are equivalent only when $\alpha = 0$. We further discuss their nonreciprocity condi-

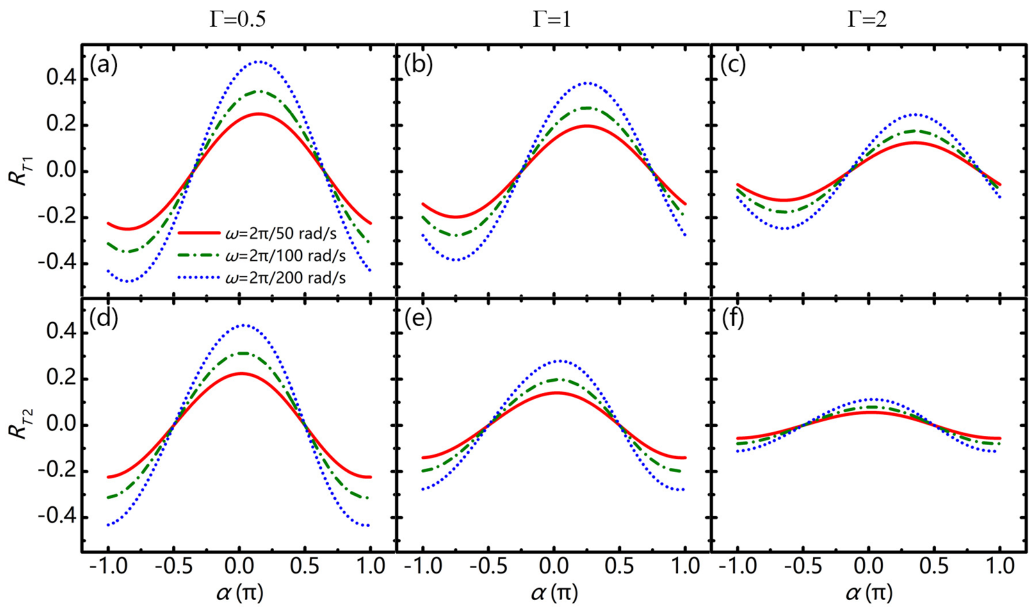

FIG. 3. R_{T1} and R_{T2} as functions of α. The parameters are the same as those for Fig. 2.

tions and define a rectification ratio (R_T or R_J) based on the reciprocal of spatial decay rate ($1/\xi$).

III. SIMULATION

We then perform simulations with COMSOL Multiphysics to confirm the theoretical analyses. For this purpose, we study the thermal conduction in a one-dimensional structure whose parameters are spatiotemporally modulated as described by Eq. (2) with $\Gamma = 1$. To ensure accuracy, the mesh size is 1/10th of the modulation wavelength (γ), and the time tolerance is 10^{-6}.

We first discuss the backward-1 case which requires to change the source position but keep the modulation direction [see Fig. 1(b)]. As theoretically predicted [Eq. (11)], $R_{T1} = 0$ occurs when $\alpha = \pi/4 \pm \pi/2$. For brevity, we set $\alpha = -\pi/4$ to perform simulations. The temperature and heat flux evolutions are presented in Figs. 4(a) and 4(c), respectively. We can clearly observe that the forward and backward-1 propagations are the same, indicating reciprocal propagations. Moreover, R_{T1} reaches the maximum value when $\alpha = \pi/4$ as predicted. We also perform simulations with $\alpha = \pi/4$, and the results are presented in Figs. 4(b) and 4(d). Clearly, the temperature amplitudes are different, indicating nonreciprocal propagations. The theoretical prediction of the forward and backward-1 temperature amplitudes are 5.13 and 1.87 K, respectively. The simulations show that the forward and backward-1 temperature amplitudes are 5.23 and 1.92 K, respectively. Therefore, the simulations agree well with the theoretical predictions.

We then discuss the backward-2 case which requires to change the modulation direction but keep the source position [see Fig. 1(c)]. Equation (11)] tells that $R_{T2} = 0$ appears when $\alpha = \pm\pi/2$, and we set $\alpha = -\pi/2$ to perform simulations [see Figs. 5(a) and 5(c)]. The forward and backward-2 propagations have the same temperature (or heat flux) ampli-

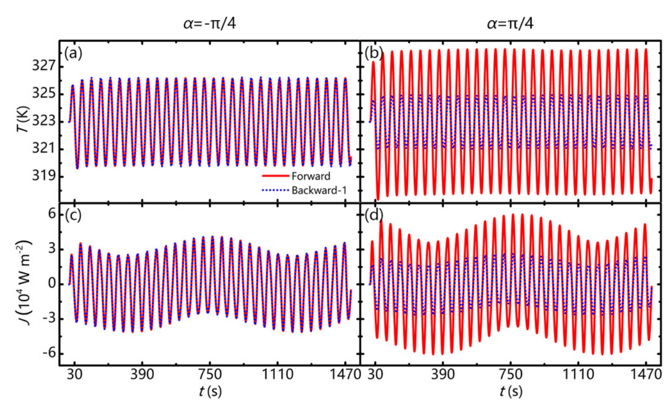

FIG. 4. Simulations of the backward-1 case. The parameters are the same as those for Fig. 2 with $\Gamma = 1$ and $L = 0.2$ m. The periodic temperature is set at $T_p = 40\cos(-2\pi t/50) + 323$ K. The detected position locates at the center of the structure. [(a) and (b)] Temperature evolution. [(c) and (d)] Heat flux evolution.

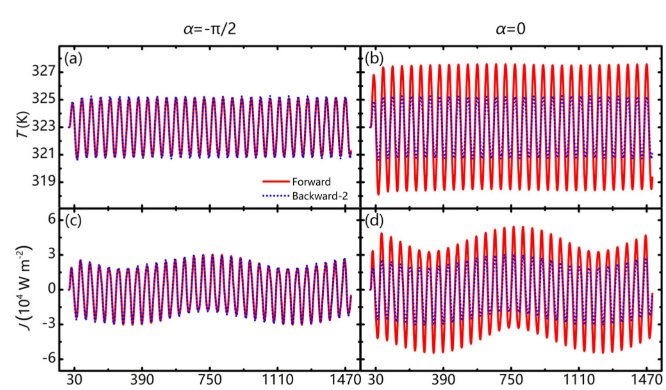

FIG. 5. Simulations of the backward-2 case. The parameters are the same as those for Fig. 4. The difference from Fig. 4 is that here we change the modulation speed instead of changing the source position.

tudes, indicating reciprocal thermal waves. In addition, R_{T2} reaches the maximum value when $\alpha = 0$ as predicted, and the simulation results are presented in Figs. 5(b) and 5(d). The theoretical prediction of the forward and backward-2 temperature amplitudes are 4.48 and 2.19 K, respectively. The simulations demonstrate that the forward and backward-1 temperature amplitudes are 4.53 and 2.24 K, respectively. Again, the simulations and theories have good agreement.

IV. DISCUSSION AND CONCLUSION

We finally provide some experimental suggestions to ensure the feasibility of practical implementations. The most crucial is to realize spatiotemporal modulations of σ (thermal conductivity) and ρ (the product of mass density and heat capacity). We first discuss the spatiotemporal modulation of σ. A large number of studies have shown that thermal conductivities can be flexibly controlled by external fields like electric fields [35,36] and light fields [37]. The in-plane thermal conductivity can change two orders of magnitude with an out-of-plane electric field [35]. We then discuss the spatiotemporal modulation of ρ by considering that of heat capacity. Many materials have a phase change [38] in the presence of an electric field, so heat capacities change with the phase change. Therefore, spatiotemporal modulations of σ and ρ can be realized with an electric field in principle. Moreover, Ref. [19] also provides an insight to practical implementations, though the experiments were conducted in electrics. Since thermotics and electrics follow similar equations (thermal conductivity corresponds to electric conductivity and heat capacity corresponds to electric capacity), spatiotemporal modulations of σ and ρ might also be realized by rotating disks, as presented in Ref. [19]. A periodic temperature can be obtained by directly using a pulse heat source or alternately using a ceramic heater and a semiconductor cooler. Therefore, these results should be possible to be experimentally validated. Thermal waves discussed in this work are based on the Fourier law, and many other kinds of thermal waves remain further explored, i.e., those considering thermal relaxation [39–42].

In summary, we propose the mechanism of tunable thermal wave nonreciprocity with spatiotemporal modulation. The tunability lies in the phase difference (α) between two spatiotemporally modulated parameters. We reveal that the homogenized thermal conductivity ($\tilde{\sigma}$) and the homogenized product of mass density and heat capacity ($\tilde{\rho}$) are independent of the phase difference (α), but the convective term (C) and the Willis term (S) are crucially dependent on the phase difference (α). We also discuss two different backward cases: (i) changing the source position and (ii) changing the modulation direction. The two cases are equivalent only when $\alpha = 0$. We further define a rectification ratio (R_{T1} or R_{T2}) based on the reciprocal of spatial decay rate ($1/\xi$) and discuss nonreciprocity conditions. These theoretical analyses are all confirmed by finite-element simulations, and experimental suggestions are also given to ensure feasibility. These results broaden the research ideas on thermal diodes [43–46], and have potential applications in thermal camouflaging [47–50] and thermal sensing [51–54].

ACKNOWLEDGMENTS

We thank Prof. Rong-Gen Cai both for suggesting us to study the role of time-dependent thermal conductivities and for helping us to improve the manuscript by raising some constructive suggestions. We acknowledge financial support from the National Natural Science Foundation of China under Grants No. 11725521 and No. 12035004, and from the Science and Technology Commission of Shanghai Municipality under Grant No. 20JC1414700.

APPENDIX

We consider two variable substitutions of $n = x - ut$ and $\tau = t$, yielding $\partial/\partial x = \partial/\partial n$ and $\partial/\partial t = \partial/\partial \tau - u\partial/\partial n$. Equation (1) can then be reduced to

$$\rho(n)\frac{\partial T}{\partial \tau} - u\rho(n)\frac{\partial T}{\partial n} + \frac{\partial}{\partial n}\left[-\sigma(n)\frac{\partial T}{\partial n}\right] = 0. \tag{A1}$$

Similarly, Eq. (2) can also be simplified as

$$\sigma(n) = \sigma_A + \sigma_B \cos(Kn), \tag{A2a}$$

$$\rho(n) = \rho_A + \rho_B \cos(Kn + \alpha). \tag{A2b}$$

We rewrite Eq. (A2) with the Fourier expansion,

$$\sigma(n) = \sum_{s=0,\,\pm 1} \sigma_s e^{iK_s n} = \sigma_0 e^{iK_0 n} + \sigma_{+1} e^{iK_{+1} n} + \sigma_{-1} e^{iK_{-1} n}, \tag{A3a}$$

$$\rho(n) = \sum_{s=0,\,\pm 1} \rho_s e^{iK_s n} = \rho_0 e^{iK_0 n} + \rho_{+1} e^{iK_{+1} n} + \rho_{-1} e^{iK_{-1} n}, \tag{A3b}$$

with $K_0 = 0$, $K_{\pm 1} = \pm K$, $\sigma_0 = \sigma_A$, $\sigma_{\pm 1} = \sigma_B/2$, $\rho_0 = \rho_A$, and $\rho_{\pm 1} = e^{\pm i\alpha}\rho_B/2$.

With the Bloch theorem, we can express the temperature solution as

$$T(n,\ \tau) = \phi(n)e^{i(Gn - W\tau)} = \left(\sum_{s=0,\,\pm 1} \phi_s e^{iK_s n}\right) e^{i(Gn - W\tau)}$$
$$= (\phi_0 e^{iK_0 n} + \phi_{+1} e^{iK_{+1} n} + \phi_{-1} e^{iK_{-1} n}) e^{i(Gn - W\tau)}, \tag{A4}$$

where G and W are the wave number and circular frequency in the n-τ frame and $\phi(n)$ is the amplitude modulation function.

We can then express $\partial T/\partial \tau$ and $\partial T/\partial n$ as

$$\frac{\partial T}{\partial \tau} = -iW(\phi_0 e^{iK_0 n} + \phi_{+1} e^{iK_{+1} n} + \phi_{-1} e^{iK_{-1} n}) e^{i(Gn - W\tau)}, \tag{A5}$$

$$\frac{\partial T}{\partial n} = i[(G + K_0)\phi_0 e^{iK_0 n} + (G + K_{+1})\phi_{+1} e^{iK_{+1} n} + (G + K_{-1})\phi_{-1} e^{iK_{-1} n}] e^{i(Gn - W\tau)}. \tag{A6}$$

We can further write $\rho(n)\partial T/\partial\tau$ as

$$\begin{aligned}\rho(n)\frac{\partial T}{\partial\tau} =& -iW(\rho_0\phi_0+\rho_{+1}\phi_{-1}+\rho_{-1}\phi_{+1})e^{iK_0n}e^{i(Gn-W\tau)}\\&-iW(\rho_0\phi_{+1}+\rho_{+1}\phi_0)e^{iK_{+1}n}e^{i(Gn-W\tau)}\\&-iW(\rho_0\phi_{-1}+\rho_{-1}\phi_0)e^{iK_{-1}n}e^{i(Gn-W\tau)}\\&+o(e^{iK_{\pm1}n}).\end{aligned}\tag{A7}$$

We can also express $-u\rho(n)\partial T/\partial n$ and $-\sigma(n)\partial T/\partial n$ as

$$\begin{aligned}-u\rho(n)\frac{\partial T}{\partial n} =& -iu[\rho_0(G+K_0)\phi_0+\rho_{+1}(G+K_{-1})\phi_{-1}+\rho_{-1}(G+K_{+1})\phi_{+1}]e^{iK_0n}e^{i(Gn-W\tau)}\\&-iu[\rho_0(G+K_{+1})\phi_{+1}+\rho_{+1}(G+K_0)\phi_0]e^{iK_{+1}n}e^{i(Gn-W\tau)}\\&-iu[\rho_0(G+K_{-1})\phi_{-1}+\rho_{-1}(G+K_0)\phi_0]e^{iK_{-1}n}e^{i(Gn-W\tau)}\\&+o(e^{iK_{\pm1}n}),\end{aligned}\tag{A8}$$

$$\begin{aligned}-\sigma(n)\frac{\partial T}{\partial n} =& -i[\sigma_0(G+K_0)\phi_0+\sigma_{+1}(G+K_{-1})\phi_{-1}+\sigma_{-1}(G+K_{+1})\phi_{+1}]e^{iK_0n}e^{i(Gn-W\tau)}\\&-i[\sigma_0(G+K_{+1})\phi_{+1}+\sigma_{+1}(G+K_0)\phi_0]e^{iK_{+1}n}e^{i(Gn-W\tau)}\\&-i[\sigma_0(G+K_{-1})\phi_{-1}+\sigma_{-1}(G+K_0)\phi_0]e^{iK_{-1}n}e^{i(Gn-W\tau)}\\&+o(e^{iK_{\pm1}n}).\end{aligned}\tag{A9}$$

With Eq. (A9), we can further derive

$$\begin{aligned}\frac{\partial}{\partial n}\left[-\sigma(n)\frac{\partial T}{\partial n}\right] =& (G+K_0)[\sigma_0(G+K_0)\phi_0+\sigma_{+1}(G+K_{-1})\phi_{-1}+\sigma_{-1}(G+K_{+1})\phi_{+1}]e^{iK_0n}e^{i(Gn-W\tau)}\\&+(G+K_{+1})[\sigma_0(G+K_{+1})\phi_{+1}+\sigma_{+1}(G+K_0)\phi_0]e^{iK_{+1}n}e^{i(Gn-W\tau)}\\&+(G+K_{-1})[\sigma_0(G+K_{-1})\phi_{-1}+\sigma_{-1}(G+K_0)\phi_0]e^{iK_{-1}n}e^{i(Gn-W\tau)}\\&+o(e^{iK_{\pm1}n}).\end{aligned}\tag{A10}$$

By arranging the terms associated with e^{iK_0n}, $e^{iK_{+1}n}$, and $e^{iK_{-1}n}$ in Eqs. (A7), (A8), and (A10) together, we can obtain three equations,

$$\begin{aligned}&-i[\rho_0(W+uG+uK_0)\phi_0+\rho_{+1}(W+uG+uK_{-1})\phi_{-1}+\rho_{-1}(W+uG+uK_{+1})\phi_{+1}]\\&+(G+K_0)[\sigma_0(G+K_0)\phi_0+\sigma_{+1}(G+K_{-1})\phi_{-1}+\sigma_{-1}(G+K_{+1})\phi_{+1}]=0,\end{aligned}\tag{A11a}$$

$$\begin{aligned}&-i[\rho_0(W+uG+uK_{+1})\phi_{+1}+\rho_{+1}(W+uG+uK_0)\phi_0]\\&+(G+K_{+1})[\sigma_0(G+K_{+1})\phi_{+1}+\sigma_{+1}(G+K_0)\phi_0]=0,\end{aligned}\tag{A11b}$$

$$\begin{aligned}&-i[\rho_0(W+uG+uK_{-1})\phi_{-1}+\rho_{-1}(W+uG+uK_0)\phi_0]\\&+(G+K_{-1})[\sigma_0(G+K_{-1})\phi_{-1}+\sigma_{-1}(G+K_0)\phi_0]=0.\end{aligned}\tag{A11c}$$

Equation (A11) is written in the n-τ frame, and we can also express it in the x-t frame by taking $k=G$ and $\omega=W+uG$, where k and ω are, respectively, the wave vector and circular frequency in the x-t frame,

$$\begin{aligned}&-i[\rho_0(\omega+uK_0)\phi_0+\rho_{+1}(\omega+uK_{-1})\phi_{-1}+\rho_{-1}(\omega+uK_{+1})\phi_{+1}]\\&+(k+K_0)[\sigma_0(k+K_0)\phi_0+\sigma_{+1}(k+K_{-1})\phi_{-1}+\sigma_{-1}(k+K_{+1})\phi_{+1}]=0,\end{aligned}\tag{A12a}$$

$$\begin{aligned}&-i[\rho_0(\omega+uK_{+1})\phi_{+1}+\rho_{+1}(\omega+uK_0)\phi_0]\\&+(k+K_{+1})[\sigma_0(k+K_{+1})\phi_{+1}+\sigma_{+1}(k+K_0)\phi_0]=0,\end{aligned}\tag{A12b}$$

$$\begin{aligned}&-i[\rho_0(\omega+uK_{-1})\phi_{-1}+\rho_{-1}(\omega+uK_0)\phi_0]\\&+(k+K_{-1})[\sigma_0(k+K_{-1})\phi_{-1}+\sigma_{-1}(k+K_0)\phi_0]=0.\end{aligned}\tag{A12c}$$

With Eqs. (A12b) and (A12c), we can derive the expressions of ϕ_{+1} and ϕ_{-1},

$$\phi_{+1} = -\frac{(k+K_{+1})\sigma_{+1}(k+K_0)-i\rho_{+1}(\omega+uK_0)}{(k+K_{+1})\sigma_0(k+K_{+1})-i\rho_0(\omega+uK_{+1})}\phi_0,\tag{A13a}$$

$$\phi_{-1} = -\frac{(k+K_{-1})\sigma_{-1}(k+K_0)-i\rho_{-1}(\omega+uK_0)}{(k+K_{-1})\sigma_0(k+K_{-1})-i\rho_0(\omega+uK_{-1})}\phi_0.\tag{A13b}$$

We then consider two approximations of $k \ll K$ and $\omega \ll uK$, so Eq. (A13) can be reduced to

$$\phi_{+1} = -\frac{K_{+1}\sigma_{+1}k - i\rho_{+1}\omega}{K_{+1}\sigma_0 K_{+1} - i\rho_0 u K_{+1}}\phi_0, \quad \text{(A14a)}$$

$$\phi_{-1} = -\frac{K_{-1}\sigma_{-1}k - i\rho_{-1}\omega}{K_{-1}\sigma_0 K_{-1} - i\rho_0 u K_{-1}}\phi_0. \quad \text{(A14b)}$$

Similarly, Eq. (A12a) can also be reduced to

$$k^2\sigma_0\phi_0 - i\omega\rho_0\phi_0 + (k\sigma_{-1}K_{+1} - i\rho_{-1}uK_{+1})\phi_{+1} + (k\sigma_{+1}K_{-1} - i\rho_{+1}uK_{-1})\phi_{-1} = 0. \quad \text{(A15)}$$

The substitution of Eq. (A14) into Eq. (A15) yields

$$k^2\sigma_0\phi_0 - i\omega\rho_0\phi_0 - \frac{(k\sigma_{-1}K_{+1} - i\rho_{-1}uK_{+1})(K_{+1}\sigma_{+1}k - i\rho_{+1}\omega)}{K_{+1}\sigma_0 K_{+1} - i\rho_0 u K_{+1}}\phi_0 - \frac{(k\sigma_{+1}K_{-1} - i\rho_{+1}uK_{-1})(K_{-1}\sigma_{-1}k - i\rho_{-1}\omega)}{K_{-1}\sigma_0 K_{-1} - i\rho_0 u K_{-1}}\phi_0 = 0. \quad \text{(A16)}$$

Equation (A16) can be further arranged in a physical form,

$$-i\omega\left(\rho_0 + \frac{iKu\rho_{+1}\rho_{-1}}{\sigma_0 K^2 - i\rho_0 uK} + \frac{-iKu\rho_{+1}\rho_{-1}}{\sigma_0 K^2 + i\rho_0 uK}\right)\phi_0 + ik\left(\frac{K^2u\sigma_{+1}\rho_{-1}}{\sigma_0 K^2 - i\rho_0 uK} + \frac{K^2u\sigma_{-1}\rho_{+1}}{\sigma_0 K^2 + i\rho_0 uK}\right)\phi_0 + k^2\left(\sigma_0 - \frac{K^2\sigma_{+1}\sigma_{-1}}{\sigma_0 K^2 - i\rho_0 uK} - \frac{K^2\sigma_{+1}\sigma_{-1}}{\sigma_0 K^2 + i\rho_0 uK}\right)\phi_0 - \omega k\left(\frac{-iK\rho_{+1}\sigma_{-1}}{\sigma_0 K^2 - i\rho_0 uK} + \frac{iK\rho_{-1}\sigma_{+1}}{\sigma_0 K^2 + i\rho_0 uK}\right)\phi_0 = 0. \quad \text{(A17)}$$

By taking $\partial/\partial t = -i\omega$, $\partial/\partial x = ik$, and $\tilde{T} = \phi_0 e^{i(kx-\omega t)}$, we can rewrite Eq. (A17) as

$$\tilde{\rho}\frac{\partial\tilde{T}}{\partial t} + C\frac{\partial\tilde{T}}{\partial x} - \tilde{\sigma}\frac{\partial^2\tilde{T}}{\partial x^2} - S\frac{\partial^2\tilde{T}}{\partial x\partial t} = 0, \quad \text{(A18)}$$

where the homogenized parameters take the form of

$$\tilde{\sigma} = \sigma_0 - \frac{K^2\sigma_{+1}\sigma_{-1}}{\sigma_0 K^2 - i\rho_0 uK} - \frac{K^2\sigma_{+1}\sigma_{-1}}{\sigma_0 K^2 + i\rho_0 uK}, \quad \text{(A19a)}$$

$$\tilde{\rho} = \rho_0 + \frac{iKu\rho_{+1}\rho_{-1}}{\sigma_0 K^2 - i\rho_0 uK} + \frac{-iKu\rho_{+1}\rho_{-1}}{\sigma_0 K^2 + i\rho_0 uK}, \quad \text{(A19b)}$$

$$C = \frac{K^2u\sigma_{+1}\rho_{-1}}{\sigma_0 K^2 - i\rho_0 uK} + \frac{K^2u\sigma_{-1}\rho_{+1}}{\sigma_0 K^2 + i\rho_0 uK}, \quad \text{(A19c)}$$

$$S = \frac{-iK\sigma_{-1}\rho_{+1}}{\sigma_0 K^2 - i\rho_0 uK} + \frac{iK\sigma_{+1}\rho_{-1}}{\sigma_0 K^2 + i\rho_0 uK}. \quad \text{(A19d)}$$

We can further reduce Eq. (A19) to

$$\tilde{\sigma} = \sigma_A\left(1 - \frac{2\pi^2\sigma_B^2}{4\pi^2\sigma_A^2 + \rho_A^2u^2\gamma^2}\right), \quad \text{(A20a)}$$

$$\tilde{\rho} = \rho_A\left(1 - \frac{1}{2}\frac{\rho_B^2u^2\gamma^2}{4\pi^2\sigma_A^2 + \rho_A^2u^2\gamma^2}\right), \quad \text{(A20b)}$$

$$C = u\frac{2\pi^2\sigma_A\sigma_B\rho_B}{4\pi^2\sigma_A^2 + \rho_A^2u^2\gamma^2}\left(\cos\alpha + \frac{\rho_A u\gamma}{2\pi\sigma_A}\sin\alpha\right), \quad \text{(A20c)}$$

$$S = u\frac{1}{2}\frac{\gamma^2\sigma_B\rho_A\rho_B}{4\pi^2\sigma_A^2 + \rho_A^2u^2\gamma^2}\left(\cos\alpha + \frac{2\pi\sigma_A}{\rho_A u\gamma}\sin\alpha\right), \quad \text{(A20d)}$$

or

$$\tilde{\sigma} = \sigma_A\left(1 - \frac{\sigma_B^2}{2\sigma_A^2}\frac{1}{1+\Gamma^2}\right), \quad \text{(A21a)}$$

$$\tilde{\rho} = \rho_A\left(1 - \frac{\rho_B^2}{2\rho_A^2}\frac{\Gamma^2}{1+\Gamma^2}\right), \quad \text{(A21b)}$$

$$C = u\frac{\sigma_B\rho_B}{2\sigma_A}\frac{1}{1+\Gamma^2}(\cos\alpha + \Gamma\sin\alpha), \quad \text{(A21c)}$$

$$S = \frac{1}{u}\frac{\sigma_B\rho_B}{2\rho_A}\frac{\Gamma^2}{1+\Gamma^2}\left(\cos\alpha + \frac{1}{\Gamma}\sin\alpha\right), \quad \text{(A21d)}$$

with $\Gamma = \rho_A u\gamma/(2\pi\sigma_A)$.

[1] Z. F. Yu and S. H. Fan, Complete optical isolation created by indirect interband photonic transitions, Nat. Photon. **3**, 91 (2009).

[2] D. L. Sounas, C. Caloz, and A. Alù, Giant non-reciprocity at the subwavelength scale using angular momentum-biased metamaterials, Nat. Commun. **4**, 2407 (2013).

[3] D. L. Sounas and A. Alù, Angular-momentum-biased nanorings to realize magnetic-free integrated optical isolation, ACS Photon. **1**, 198 (2014).

[4] D. L. Sounas and A. Alù, Non-reciprocal photonics based on time modulation, Nat. Photon. **11**, 774 (2017).

[5] A. Mock, D. Sounas, and A. Alù, Magnet-free circulator based on spatiotemporal modulation of photonic crystal defect cavities, ACS Photon. **6**, 2056 (2019).

[6] R. Fleury, D. L. Sounas, and A. Alù, Subwavelength ultrasonic circulator based on spatiotemporal modulation, Phys. Rev. B **91**, 174306 (2015).

[7] C. Shen, J. F. Li, Z. T. Jia, Y. B. Xie, and S. A. Cummer, Nonreciprocal acoustic transmission in cascaded resonators via spatiotemporal modulation, Phys. Rev. B **99**, 134306 (2019).

[8] C. Shen, X. H. Zhu, J. F. Li, and S. A. Cummer, Nonreciprocal acoustic transmission in space-time modulated coupled resonators, Phys. Rev. B **100**, 054302 (2019).

[9] X. H. Zhu, J. F. Li, C. Shen, X. Y. Peng, A. L. Song, L. Q. Li, and S. A. Cummer, Non-reciprocal acoustic transmission via space-time modulated membranes, Appl. Phys. Lett. **116**, 034101 (2020).

[10] J. W. Zang, D. Correas-Serrano, J. T. S. Do, X. Liu, A. Alvarez-Melcon, and J. S. Gomez-Diaz, Nonreciprocal Wavefront Engineering with Time-Modulated Gradient Metasurfaces, Phys. Rev. Appl. **11**, 054054 (2019).

[11] X. X. Guo, Y. M. Ding, Y. Duan, and X. J. Ni, Nonreciprocal metasurface with space–time phase modulation, Light Sci. Appl. **8**, 123 (2019).

[12] Q. Wu, H. Chen, H. Nassar, and G. L. Huang, Non-reciprocal Rayleigh wave propagation in space–time modulated surface, J. Mech. Phys. Solids **146**, 104196 (2021).

[13] S. P. Wallen and M. R. Haberman, Nonreciprocal wave phenomena in spring-mass chains with effective stiffness modulation induced by geometric nonlinearity, Phys. Rev. E **99**, 013001 (2019).

[14] Y. Y. Chen, X. P. Li, H. Nassar, A. N. Norris, C. Daraio, and G. L. Huang, Nonreciprocal wave propagation in a continuum-based metamaterial with space-time modulated resonators, Phys. Rev. Appl. **11**, 064052 (2019).

[15] H. N. Li, H. Moussa, D. Sounas, and A. Alù, Parity-Time Symmetry Based on Time Modulation, Phys. Rev. Appl. **14**, 031002(R) (2020).

[16] V. Ramakrishnan and M. J. Frazier, Transition waves in multistable metamaterials with space-time modulated potentials, Appl. Phys. Lett. **117**, 151901 (2020).

[17] B. Edwards and N. Engheta, Asymmetrical diffusion through time-varying material parameters, in *Proceedings of the Conference on Lasers and Electro-Optics* (Optical Society of America, 2017).

[18] D. Torrent, O. Poncelet, and J.-C. Batsale, Nonreciprocal Thermal Material by Spatiotemporal Modulation, Phys. Rev. Lett. **120**, 125501 (2018).

[19] M. Camacho, B. Edwards, and N. Engheta, Achieving asymmetry and trapping in diffusion with spatiotemporal metamaterials, Nat. Commun. **11**, 3733 (2020).

[20] M. Farhat, P.-Y. Chen, H. Bagci, C. Amra, S. Guenneau, and A. Alù, Thermal invisibility based on scattering cancellation and mantle cloaking, Sci. Rep. **5**, 9876 (2015).

[21] R. Mulaveesala and S. Tuli, Theory of frequency modulated thermal wave imaging for nondestructive subsurface defect detection, Appl. Phys. Lett. **89**, 191913 (2006).

[22] R. Mulaveesala and S. Tuli, Applications of frequency modulated thermal wave imaging for nondestructive characterization, AIP Conf. Proc. **1004**, 15 (2008).

[23] S. Tuli and K. Chatterjee, Frequency modulated thermal wave imaging, AIP Conf. Proc. **1430**, 523 (2012).

[24] Y. Li, Y.-G. Peng, L. Han, M.-A. Miri, W. Li, M. Xiao, X.-F. Zhu, J. L. Zhao, A. Alù, S. H. Fan, and C.-W. Qiu, Anti-parity-time symmetry in diffusive systems, Science **364**, 170 (2019).

[25] L. J. Xu, J. Wang, G. L. Dai, S. Yang, F. B. Yang, G. Wang, and J. P. Huang, Geometric phase, effective conductivity enhancement, and invisibility cloak in thermal convection-conduction, Int. J. Heat Mass Transf. **165**, 120659 (2021).

[26] P. C. Cao, Y. Li, Y. G. Peng, C. W. Qiu, and X. F. Zhu, High-order exceptional points in diffusive systems: Robust APT symmetry against perturbation and phase oscillation at APT symmetry breaking, ES Energy Environ. **7**, 48 (2020).

[27] L. J. Xu, G. L. Dai, G. Wang, and J. P. Huang, Geometric phase and bilayer cloak in macroscopic particle-diffusion systems, Phys. Rev. E **102**, 032140 (2020).

[28] L. J. Xu and J. P. Huang, Negative thermal transport in conduction and advection, Chin. Phys. Lett. **37**, 080502 (2020).

[29] M. Farhat, S. Guenneau, P.-Y. Chen, A. Alù, and K. N. Salama, Scattering Cancellation-Based Cloaking for the Maxwell-Cattaneo Heat Waves, Phys. Rev. Appl. **11**, 044089 (2019).

[30] L. J. Xu and J. P. Huang, Controlling thermal waves with transformation complex thermotics, Int. J. Heat Mass Transf. **159**, 120133 (2020).

[31] L. J. Xu and J. P. Huang, Active thermal wave cloak, Chin. Phys. Lett. **37**, 120501 (2020).

[32] A.-L. Chen, Z.-Y. Li, T.-X. Ma, X.-S. Li, and Y.-S. Wang, Heat reduction by thermal wave crystals, Int. J. Heat Mass Transf. **121**, 215 (2018).

[33] L. J. Xu and J. P. Huang, Thermal convection-diffusion crystal for prohibition and modulation of wave-like temperature profiles, Appl. Phys. Lett. **117**, 011905 (2020).

[34] M. Gandolfi, C. Giannetti, and F. Banfi, Temperonic Crystal: A Superlattice for Temperature Waves in Graphene, Phys. Rev. Lett. **125**, 265901 (2020).

[35] G. Z. Qin, Z. Z. Qin, S.-Y. Yue, Q.-B. Yan, and M. Hu, External electric field driving the ultra-low thermal conductivity of silicene, Nanoscale **9**, 7227 (2017).

[36] S. C. Deng, J. L. Yuan, Y. L. Lin, X. X. Yu, D. K. Ma, Y. W. Huang, R. C. Ji, G. Z. Zhang, and N. Yang, Electric-field-induced modulation of thermal conductivity in poly (vinylidene fluoride), Nano Energy **82**, 105749 (2021).

[37] J. Shin, J. Sung, M. Kang, X. Xie, B, Lee, K. M. Lee, T. J. White, C. Leal, N. R. Sottos, P. V. Braun, and D. G. Cahill, Light-triggered thermal conductivity switching in azobenzene polymers, Proc. Natl. Acad. Sci. USA **116**, 5973 (2019).

[38] N. P. Lu, P. F. Zhang, Q. H. Zhang, R. M. Qiao, Q. He, H.-B. Li, Y. J. Wang, J. W. Guo, D. Zhang, Z. Duan, Z. L. Li, M. Wang, S. Z. Yang, M. Z. Yan, E. Arenholz, S. Y. Zhou, W. L. Yang, L. Gu, C.-W. Nan, J. Wu, Y. Tokura, and P. Yu, Electric-field control of tri-state phase transformation with a selective dual-ion switch, Nature (London) **546**, 124 (2017).

[39] D. D. Joseph and L. Preziosi, Heat Waves, Rev. Mod. Phys. **61**, 41 (1989).

[40] B.-D. Nie and B.-Y. Cao, Three mathematical representations and an improved ADI method for hyperbolic heat conduction, Int. J. Heat Mass Transf. **135**, 974 (2019).

[41] M. Gandolfi, G. Benetti, C. Glorieux, C. Giannetti, and F. Banfi, Accessing temperature waves: A dispersion relation perspective, Int. J. Heat Mass Transf. **143**, 118553 (2019).

[42] M. Simoncelli, N. Marzari, and A. Cepellotti, Generalization of Fourier's law into viscous heat equations, Phys. Rev. X **10**, 011019 (2020).

[43] B. W. Li, L. Wang, and G. Casati, Thermal diode: Rectification of heat flux, Phys. Rev. Lett. **93**, 184301 (2004).

[44] Y. Li, X. Y. Shen, Z. H. Wu, J. Y. Huang, Y. X. Chen, Y. S. Ni, and J. P. Huang, Temperature-Dependent Transformation Thermotics: From Wwitchable Thermal Cloaks to Macroscopic Thermal Diodes, Phys. Rev. Lett. **115**, 195503 (2015).

[45] K. Z. Xiong, J. Zhou, M. Tang, C. H. Zeng, and Z. H. Liu, Control of thermal conduction and rectification in a model of complex networks with two asymmetric parts, Phys. Rev. E **98**, 062144 (2018).

[46] T. J. Alexander, High-heat-flux rectification due to a localized thermal diode, Phys. Rev. E **101**, 062122 (2020).

[47] Y. Li, K.-J. Zhu, Y.-G. Peng, W. Li, T. Z. Yang, H. X. Xu, H. Chen, X.-F. Zhu, S. H. Fan, and C.-W. Qiu, Thermal meta-device in analog of zero-index photonics, Nat. Mater. **18**, 48 (2019).

[48] L. J. Xu, S. Yang, and J. P. Huang, Dipole-assisted thermotics: Experimental demonstration of dipole-driven thermal invisibility, Phys. Rev. E **100**, 062108 (2019).

[49] J. X. Li, Y. Li, P.-C. Cao, T. Z. Yang, X.-F. Zhu, W. Y. Wang, and C.-W. Qiu, A continuously tunable solid-like convective thermal metadevice on the reciprocal line, Adv. Mater. **32**, 2003823 (2020).

[50] F. B. Yang, B. Y. Tian, L. J. Xu, and J. P. Huang, Experimental Demonstration of Thermal Chameleonlike Rotators with Transformation-Invariant Metamaterials, Phys. Rev. Appl. **14**, 054024 (2020).

[51] T. Z. Yang, X. Bai, D. L. Gao, L. Z. Wu, B. W. Li, J. T. Thong, and C.-W. Qiu, Invisiable sensor: Simultaneous camouflaging and sensing in multiphysical fields, Adv. Mat. **27**, 7752 (2015).

[52] T. C. Han, P. Yang, Y. Li, D. Y. Lei, B. W. Li, K. Hippalgaonkar, and C.-W. Qiu, Full-parameter omnidirectional thermal metadevices of anisotropic geometry, Adv. Mater. **30**, 1804019 (2018).

[53] P. Jin, L. J. Xu, T. Jiang, L. Zhang, and J. P. Huang, Making thermal sensors accurate and invisible with an anisotropic monolayer scheme, Int. J. Heat Mass Transf. **163**, 120437 (2020).

[54] L. J. Xu, J. P. Huang, T. Jiang, L. Zhang, and J. P. Huang, Thermally invisible sensors, Europhys. Lett. **132**, 14002 (2020).